

A Compact Rupee Shaped Dual Band Antenna for WiMAX and WLAN Applications

Praveen Naidu V
Department of E&TC
SIU (Deemed University)
Lavale,Pune-412115

Raj Kumar
Department of AE
A.R.D.E
Pashan, Pune - 411021

R.V.S. Ram Krishna
Department of Electronics
DIAT (Deemed University)
Girinagar, Pune - 411025

ABSTRACT

A compact rupee shaped CPW-fed antenna with dual-band operation for worldwide interoperability for microwave access (WiMAX) and wireless local area network (WLAN) applications is proposed in this paper. The antenna has a very simple structure and a compact size of $17 \times 17.5 \times 1.6 \text{ mm}^3$. A prototype is fabricated and then tested. The measured impedance bandwidth at VSWR 2:1 is 700 MHz from 3.2-3.9 GHz and 870 MHz from 4.7-5.57 GHz which covers the 5.2/5.8 GHz WLAN and 3.5/5.5 GHz WiMAX bands. The measured and simulated results are found to be in good agreement.

Keywords

CPW-fed, compact antenna, WiMAX, WLAN.

1. INTRODUCTION

In the recent years much attention has been paid towards the development of compact multi-band antennas with less fabrication cost and good performance characteristics for various wireless communication applications such as wireless local area network (WLAN) and worldwide interoperability for microwave access (WiMAX). Various types of multi-frequency antennas have been designed and developed over the few years, which can be used for multi-frequency operations, such as Planar Inverted F-shaped Antenna PIFA [1], monopole antenna [2], patch antenna [3], slot antenna, and others [4-6]. Out of these, printed monopole antennas are most suitable for integration on the circuit board of a communication device, which gives the attractive features of occupying very small volume of the system and decreasing the fabrication cost of the final product. From the available literature, the printed monopole antennas reported in [7-9] are capable of single-band operation only, and the printed dual-band inverted- F monopole antenna shown in [10] requires a shorting pin for ground connection, which increases the antenna complexity and the fabrication cost as well. In addition to the design using the printed monopole antenna, the printed dipole antenna for dual-band operation has also been given in [11], in which two separate dipoles of different arm lengths are printed on both sides of a dielectric substrate and the longer and shorter dipoles arms, respectively, the antenna had been designed to generate a resonant mode for operating in the 2.4 and 5.2 GHz bands.

Various designs of dual-band antennas have also been demonstrated in the recent years, For example, the antenna presented in [12] consists of a rectangular patch and straight strips with different length, and the antenna proposed in [13] comprises a direct-radiating patch and a parasitic C-shaped strip. To enhance the bandwidth, a dual wideband monopole

antenna [14] was proposed with a parasitic patch using electromagnetic coupling mechanism to cover the whole WLAN bands and WiMAX bands. However, the overall size of the antenna is somewhat large ($48 \times 58 \text{ mm}^2$), occupying much of the device space. A modified ground plane on the bottom layer further more improves the high frequency performances [15]. Some CPW-fed monopole antennas also have been proposed to meet the dual-band requirements, such as G-shaped [16] and triangle-Shaped [17-18]. The above stated prototypes usually use large ground plane and thick substrate. All the above reported antennas are good in bandwidth and radiation characteristic, while a few of them are having relatively larger size, and therefore they are very difficult to integrate with miniaturized wireless mobile communication devices.

In this paper, a compact rupee shaped Coplanar Waveguide (CPW) fed antenna design with dual-band operation is proposed, the geometry of which is described in Section 2. The antenna has a compact size and is useful for WLAN and WiMAX applications. The proposed antenna consists of a rupee shape patch, two rectangular strips extending from the rupee shape patch, and a CPW feed line. The proposed antenna was designed, optimized and tested using electromagnetic software: CST Microwave Studio based on the Finite Integration Technique (FIT). By properly selecting the dimensions of the proposed antenna, good dual-band impedance bandwidth and radiation characteristics suitable for the WLAN/WiMAX communication systems can be obtained. Measured results show that the antenna has the impedance bandwidth of 700 MHz (3.2-3.9 GHz), and 870 MHz (4.7-5.5 GHz), which can cover the 5.2 GHz WLAN bands and 3.5/5.5 GHz WiMAX bands. More Details of simulated results and behavioral analysis are presented and discussed in the following sections.

2. ANTENNA DESIGN

As shown in Figure 1, the configuration of the proposed antenna is designed, optimized, and fabricated on a 1.6 mm thick FR4 substrate having permittivity of 4.4 and loss tangent of 0.02. The overall size of the antenna is $17 \times 17.5 \times 1.6 \text{ mm}^3$. The rupee shape patch is fed by a 50Ω CPW line. Two rectangular shaped strips are employed to produce two resonant modes. The dimensions of the proposed antenna are optimized and shown in Table 1.

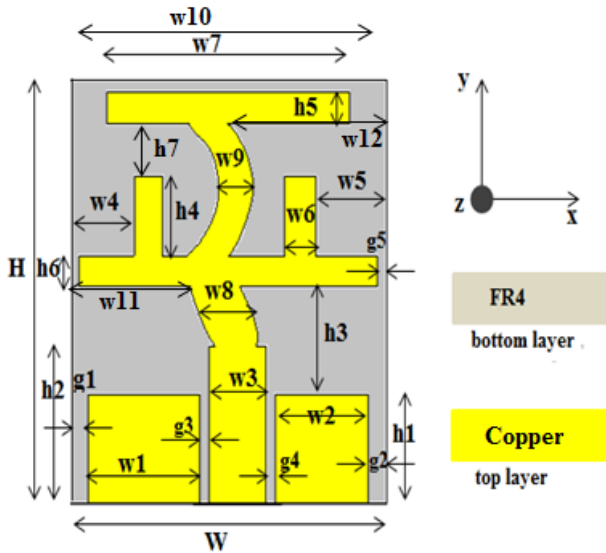
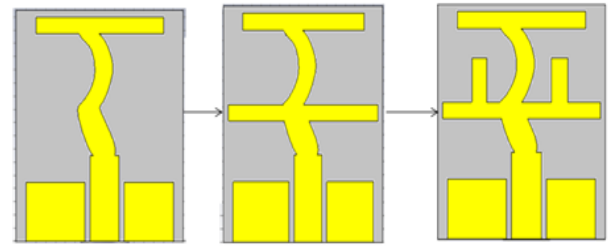


Figure 1. Geometry of the proposed dual-band antenna.

Table 1. Optimal parameters of the proposed antenna (see Figure 1)

Parameter	Value(mm)	Parameter	Value(mm)
W	17	w3	3
H	17.5	w4	3.5
w1	6	w5&w8	3.8
w2	5	w6	1.7
w7	13	h7	2.2
w9	3.1	w10	16
w11	6	h1	4.5
h2	6.5	h3	4.5
h4	3.5	h5	1.3
h6	1.2	g1&g2	1
g3&g4&g5	0.5	w12	10

The evolution process of the proposed compact antenna and the corresponding reflection coefficients (S_{11}) are shown in Figure 2(a) and Figure 2(b) respectively. The evolution process starts with the design of Antenna #1, which consists of a rupee shaped patch excited by a CPW feed. From the reflection coefficient (S_{11}) graph given in Figure 2(b), the first resonant mode frequency is observed at around 3.5 GHz and Antenna #1 covers the operating band from 3.3-3.89 GHz. Next, a rectangular strip is added to Antenna #1 (Antenna #2) to excite a second resonant mode frequency at around 5.85 GHz. From the reflection coefficient (S_{11}) graph given in Figure 2(b), Antenna #2 has impedance bandwidths of 3.3-3.85 GHz and 5.75-6.25 GHz with resonances at 3.6 GHz and 5.85 GHz respectively. Finally, in order to tune and increase the bandwidth of second resonant mode, two small rectangular strips are added to Antenna #2 (Proposed antenna). From the reflection coefficient (S_{11}) graph given in Figure 2(b), the proposed antenna has impedance bandwidths of 3.3-3.9 GHz and 5.0-6.3 GHz with resonances at 3.5 GHz and 5.8 GHz. This can both cover the 5.2 GHz WLAN band and the 3.5/5.5 GHz WiMAX band.



Antenna #1 Antenna #2 Proposed antenna
Figure 2(a) The evolution process of the proposed antenna.

The resonances seen in the final version of the antenna can be attributed to the combination of different parts (stubs) of the antenna structure behaving like a monopole. In particular, the first two resonance frequencies can be given by equations (1) and (2).

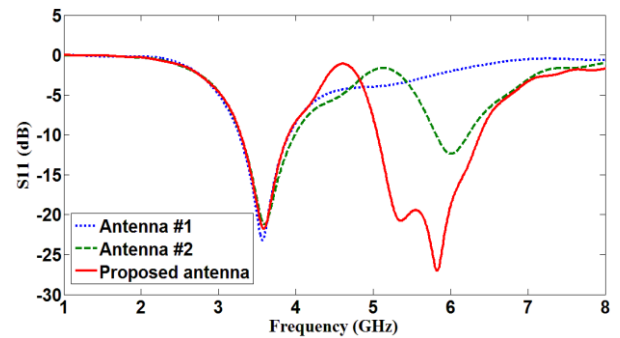


Figure 2(b). Simulated reflection coefficient of different structures involved in the design.

$$f_1 = \frac{c}{4l_1\sqrt{\epsilon_{r,eff}}} \quad (1)$$

$$f_1 = \frac{c}{4l_2\sqrt{\epsilon_{r,eff}}} \quad (2)$$

$$l_1 = h_3 + h_4 + h_5 + h_6 + h_7 \quad (3)$$

$$l_2 = h_3 + h_6 + w_{11} - w_4 \quad (4)$$

$$\epsilon_{r,eff} = \frac{\epsilon_r + 1}{2} \quad (5)$$

Here, c stands for the velocity of light in free space, l_1 and l_2 are the effective monopole heights in the two cases obtained as shown in equations (3) and (4) while $\epsilon_{r,eff}$ is the effective relative permittivity to be calculated from equation (5). For calculating the effective relative permittivity, it is assumed that for a CPW fed monopole, half of the established field lies in air while the remaining half is distributed in the substrate. The calculated resonance frequencies using equations (1) to (5) and using the dimensions given in Table 1 are compared against the simulated values in Table 2.

Table 2. Calculated and Simulated Resonances

Resonance	Effective Height	Calculated Value	Simulated Value
f_1	$l_1 = 12.7$ mm	3.6 GHz	3.5 GHz
f_2	$l_2 = 8.2$ mm	5.57 GHz	5.2 GHz

The surface current distribution for the proposed antenna at four different frequencies are given in the Figure 3. In the figure, the red colour indicates maximum current density while blue colour indicates minimum current density. For the first resonant mode, a large surface current density is observed along the rupee shaped patch, whereas for other resonant modes, current distribution becomes more concentrated along the rectangular strips and rupee shaped patch. The current distribution justifies the assumptions made previously regarding the various parts of the antenna responsible for the various resonances.

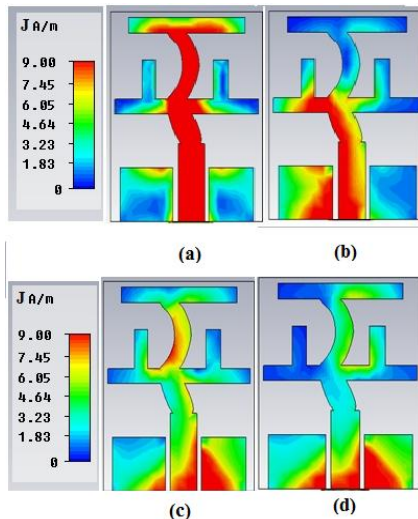


Figure 3. Simulated surface current distribution of the proposed antenna at (a) 3.5 GHz, (b) 5.2 GHz, (c) 5.5 GHz, (d) 5.8 GHz.

3. RESULTS AND DISCUSSION

The proposed antenna is designed and simulated using CST Microwave Studio. The antenna is then fabricated with the optimized dimensions as given in Table 1. A photograph of the fabricated antenna is shown in Figure 4. The measurements for the fabricated prototype were taken on a Rohde & Schwarz Vector Network Analyzer (ZVA-40). Figure 5 describes the simulated and measured S_{11} against the frequency for the antenna, as it can be seen from the figure, the simulated and measured results are in good agreement and the slight disagreement may be due to uncertainty in the dielectric constant of the substrate and assembly misalignments. For better understanding purpose the comparison between simulated and measured results of the proposed antenna are listed in Table 3. The measured impedance bandwidths of the antenna shown in Figure 5 for $S_{11} \leq -10$ dB are about 700 MHz (3.2-3.9 GHz) with resonance at 3.6 GHz and 870 MHz (4.7-5.57 GHz) with resonance at 5.25 GHz which can be used for the 5.2 GHz WLAN and 3.5/5 GHz WiMAX bands.

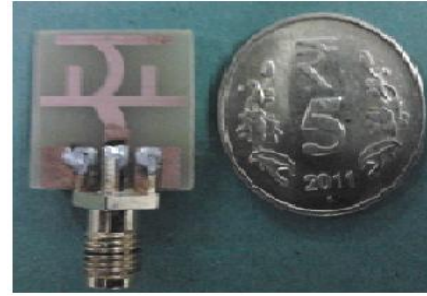


Figure 4. Photograph of the proposed antenna

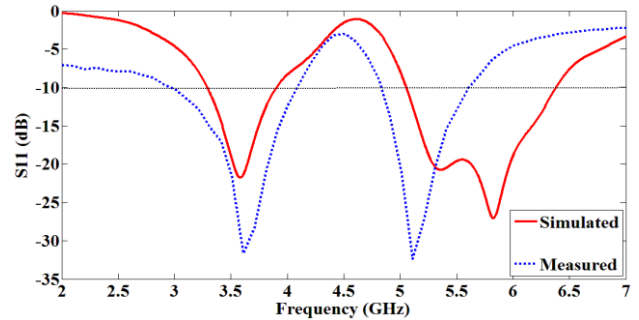


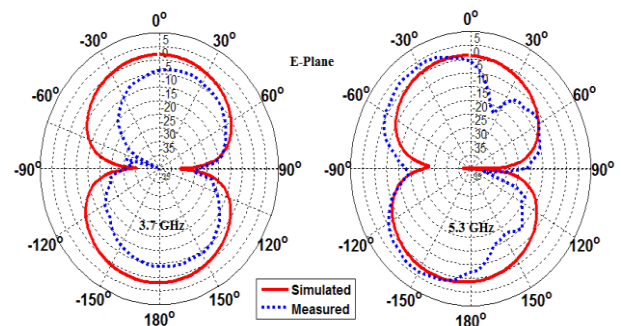
Figure 5. Measured and simulated reflection coefficient of the proposed antenna.

Table 3. Measured and simulated impedance bandwidths of the proposed antenna.

	First resonant mode		Second resonant mode	
	f_1 (GHz)	BW (MHz)	f_2 (GHz)	BW (MHz)
Measured	3.6	800	5.25	870
Simulated	3.5	650	5.8	1303

3.1 Radiation Patterns

The radiation patterns of the proposed rupee shaped compact dual-band antenna are simulated in E and H planes using CST Microwave Studio and measured in the in-house anechoic chamber using antenna measurement system. A standard double ridged horn antenna is used as reference antenna. The simulated and measured radiation patterns are shown in Figure 6 for different frequencies. The measured and simulated results are in close agreement. The H-plane radiation has omni-directional pattern while the E-plane radiation has bidirectional (dumb bell shaped) pattern.



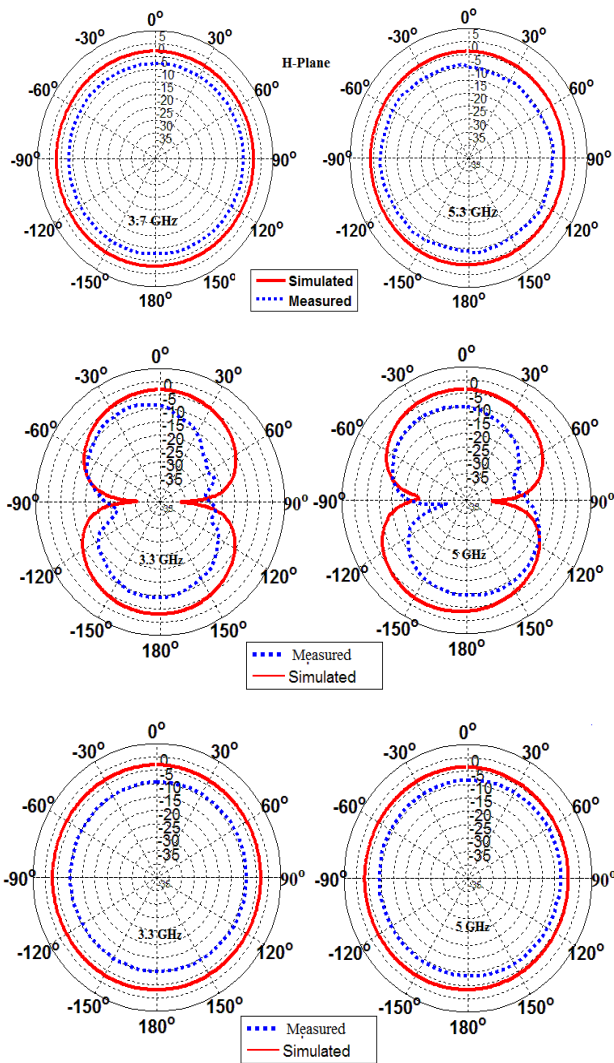


Figure 6. Measured and simulated radiation patterns of the proposed antenna at 3.7 GHz, 3.3 GHz, 5 GHz and 5.3 GHz.

For better understanding purpose the simulated beam width at different frequencies of the proposed antenna are listed in Table 4.

Table 4. Simulated beam width of the proposed antenna.

S.No	Frequency	Beam Width (3 dB)
1	3.3 GHz	84.2 deg
2	3.7 GHz	82.3 deg
3	5 GHz	89.2 deg
4	5.3 GHz	80.8 deg

4. PARAMETRIC STUDY OF THE ANTENNA

The effects of the various parameters describing the antenna geometry on the performance of the antenna are discussed in this section. In the beginning, the heights of the horizontal stubs denoted by 'h5' and 'h6' are varied and the results are shown in Figure 7 and Figure 8. In both the figures, the performance indicator considered is the reflection coefficient

of the antenna. An increase in the value of h5 causes the overall height of the monopole to increase thus reducing the first resonant frequency. The same thing is observed from Figure 7. On the other hand, an increase in the value of h6 leads to an increase in the current traversal path for the second resonance (l_2 as given by equation 4) and thus lowers the second resonant frequency. Here, it is to be noted that while varying h6, the gap (h4+h7) is reduced. Hence, there is no change in the overall height of the monopole and consequently no change in the first resonance frequency.

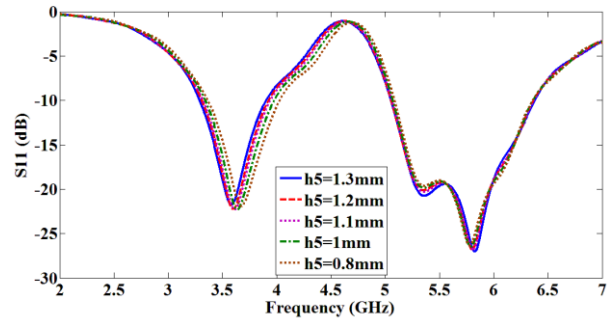


Figure 7. Effect of width 'h5' on the return loss of proposed antenna

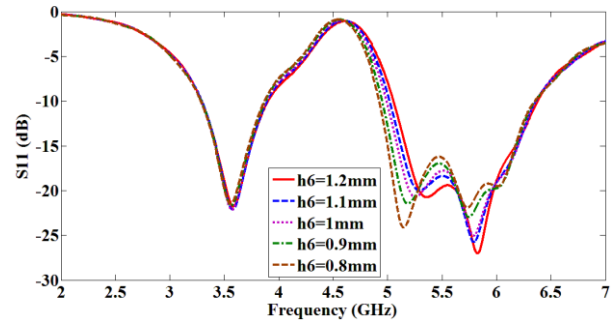


Figure 8. Effect of width 'h6' on the return loss of proposed antenna

The next parameter studied is the length of the middle horizontal stub denoted by 'w10' in Figure 1. This stub is partly responsible for the generation of the second resonance and a segment of 'w10' contributes to the value of the second resonance frequency (Equations 2 & 4). Accordingly, it is seen from Figure 9, that an increase in the value of w10 causes a reduction in the second resonant frequency (the first dip in the second band). Also it is observed that the impedance matching in the second band deteriorates with an increase in w10. In Figure 10, the effect of varying the length of the upper horizontal stub (denoted by w7) on the reflection coefficient of the antenna is shown. It can be seen from the plot of the surface current distribution (Figure 3) that there is a current spread seen on the top horizontal stub particularly at the first resonance frequency. From Figure 10, it is observed that directly or indirectly, w7 influences both the first and second resonances. A smooth reduction in the value of the first and second resonant frequencies is observed with an increase in the value of w7. No much variation is observed however in the magnitude of the return loss. The height of a small vertical stub attached to the middle horizontal stub as shown in the antenna geometry (Figure 1) is denoted by h4. The variations in the reflection coefficient with variations in h4 are shown in Figure 11. Expectedly, h4 has no major influence on the first resonance frequency and although the second resonance frequency is not affected by h4 there is noticeable improvement in the impedance matching attained

in the second band consequent to an increase in the value of h_4 .

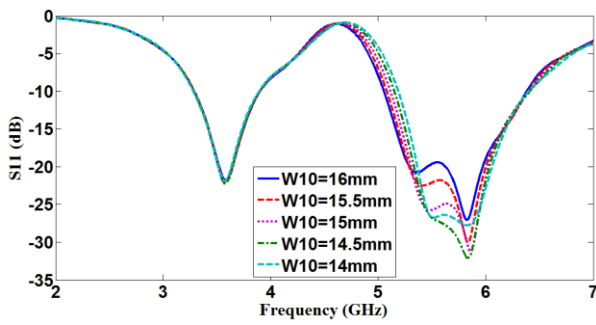


Figure 9. Effect of length 'w10' on the return loss of proposed antenna

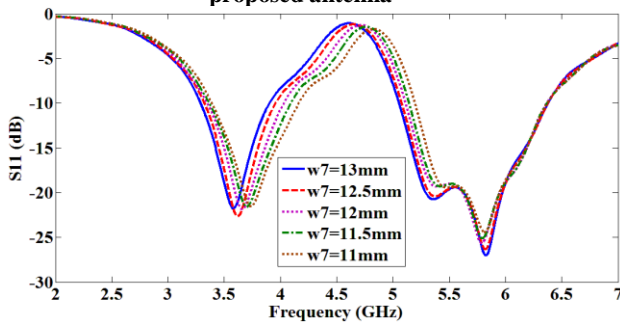


Figure 10. Effect of length 'w7' on the return loss of proposed antenna

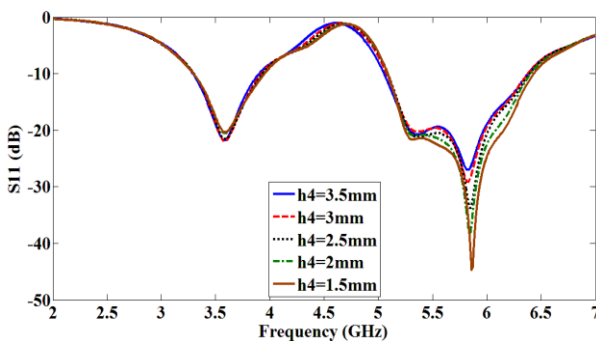


Figure 11. Effect of height 'h4' on the return loss of proposed antenna

The height h_3 is another important parameter affecting the reflection coefficient characteristics. Variation in h_3 varies the effective height of the monopole formed from the rectangular strips. From the Figure 12, it can be seen that as the height ' h_3 ' increases, the first resonant frequency shifts towards lower frequency side. Also it is seen that with an increase in h_3 , the impedance matching over the lower band deteriorates whereas the matching improves for the upper band. Hence there exists an optimal value of h_3 for good impedance matching over both the bands.

Finally, Figures 13 and 14 show the variation of return loss with a change in the gap width ' g_5 ' and ' g_1 ' respectively. As the width ' g_5 ' increases, the second resonant frequency shifts to the higher side leading to a smaller bandwidth for the second band. However there is an improvement in the impedance matching as evident from smaller return loss seen for larger values of g_5 . Hence an optimal value of g_5 is chosen while fabrication. The effect of the separation ' g_1 ' on the return loss is shown in Figure 14. It is seen that the impedance matching in the second band is affected and it improves in general with a larger value of g_1 .

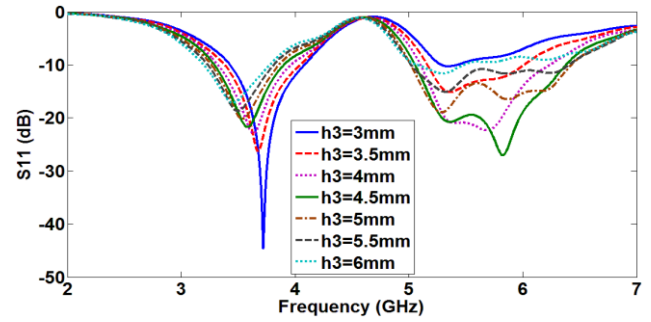


Figure 12. Effect of height 'h3' on the return loss of proposed antenna

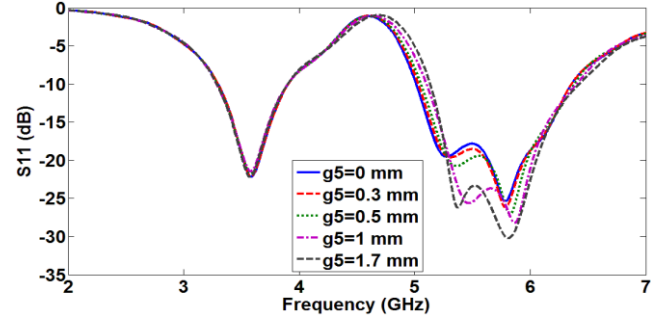


Figure 13. Effect of gap width 'g5' on the return loss of proposed antenna

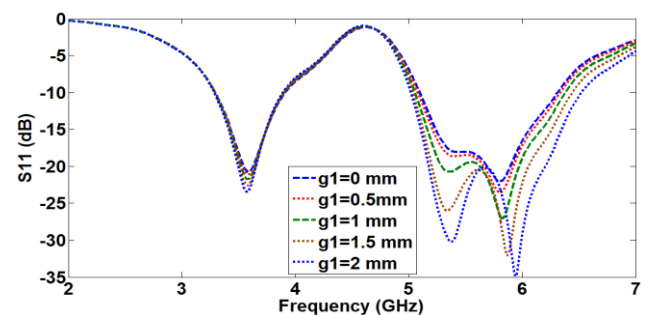


Figure 14. Effect of gap width 'g1' on the return loss of proposed antenna

5. PEAK GAIN AND RADIATION EFFICIENCY

The measured and simulated peak gain of the proposed antenna across the dual operating bands is illustrated in Figure 15. As can be seen, stable gain variations across desired bands have been achieved. The peak gain remains between 1.5-2.5dB in the useful bands while showing an increase in the high frequency region which is due to the increased effective area of the antenna at shorter wavelengths. Figure 16 shows the simulated radiation efficiencies calculated by using CST Microwave Studio for the proposed antenna.

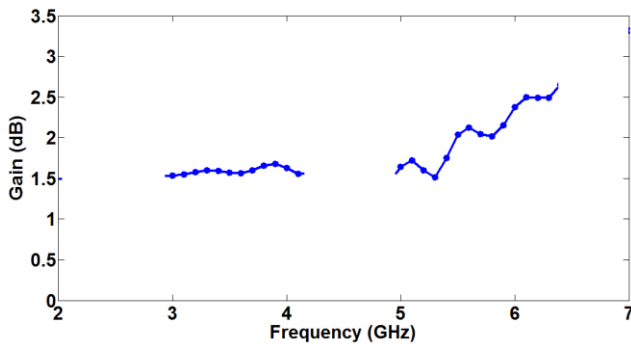


Figure 15. Simulated peak gain of the proposed antenna

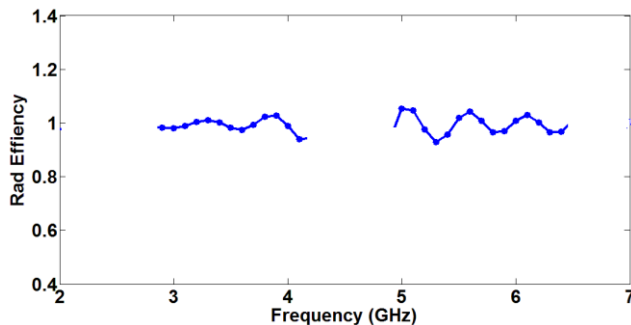


Figure 16. Simulated radiation efficiency of the proposed antenna

5. CONCLUSION

A compact rupee shape CPW-fed monopole antenna with dual-band operation for WiMAX and WLAN applications is designed and experimentally demonstrated. The proposed antenna is simple, easy to design, fabricate and can be integrate with MIC/MMICs devices. In the proposed rupee shape antenna, the rectangular strips and patch are utilized to excite two resonances into two operating bands. The antenna has been simulated using 3D electromagnetic software CST Microwave studio. The effects of various design parameters are studied thoroughly. The measured results are in good agreement with the simulated results. This compact antenna can be useful for the 5.2/5.8 GHz WLAN and 3.5/5.5 GHz WiMAX applications.

6. ACKNOWLEDGMENT

The author likes to acknowledge vice-chancellor DIAT (DU) Pune and Symbiosis International University (DU), Pune for continuous support. Author also likes to acknowledge Nagendra Kushwaha for his technical suggestions.

7. REFERENCES

- [1]. Elsadek, H. and D. M. Nashaat, "Quad band compact size trapezoidal PIFA antenna," *Journal of Electromagnetic Waves and Applications*, Vol. 21, No. 7, 865-876, 2007.
- [2]. Pan, B, R. L. Li, J. Papapolymerou, J. Laskar, and M. M. Tentzeris, "Low-profile broadband and dual-frequency two-strip planar monopole antennas" *IEEE Antennas and Propagation Society International Symposium*, 2665-2668, 2006.
- [3]. Lin, S.-J. and J.-S. Row, "Monopolar patch antenna with dual-band and wideband operations," *IEEE Transactions on Antennas and Propagation*, Vol. 56, 900-903, 2008.
- [4]. Deepu, V., K. R. Rohith, J. Manoj, M. N. Suma, K. Vasudevan, C. K. Aanandan, and P. Mohanan, "Compact uniplanar antenna for WLAN applications," *IEEE Electronic Letters*, Vol. 43, 70-72, 2007.
- [5]. Wang, F. J. and J.-S. Zhang, "Wideband cavity-backed patch antenna for PCS/IMT2000/2.4 GHz WLAN," *Progress In Electromagnetics Research*, Vol. 74, 39-46, 2007.
- [6]. Liu, W. C. and H.-J. Liu, "Miniaturized asymmetrical CPW-FED meandered strip antenna for triple-band operation," *Journal of Electromagnetic Waves and Applications*, Vol. 21, No. 8, 1089-1097, 2007.
- [7]. C. Wu, "Printed antenna structure for wireless data communications," U.S. Pat. 6 008 774, Dec. 28, 1999.
- [8]. L. M. Burns and C. L. Woo, "Dual orthogonal monopole antenna system," U.S. Pat. 5 990 838, Nov. 23, 1999.
- [9]. M. Ali and G. J. Hayes, "Analysis of integrated inverted-F antennas for bluetooth applications," in *Proc. 2000 IEEE-APS Conf. on Antennas Propagation for Wireless Communications*, Waltham, MA, pp. 21-24.
- [10]. Y. L. Kuo, T.W. Chiou, and K. L. Wong, "A novel dual-band printed inverted-F antenna," *Microwave Opt. Technol. Lett.*, vol. 31, pp. 353-355, Dec. 5, 2001.
- [11]. Y. H. Suh and K. Chang, "Low cost microstrip-fed dual frequency printed dipole antenna for wireless communications," *Electron. Lett.*, vol. 36, pp. 1177-1179, July 6, 2000.
- [12]. Ren, X.-S., Y.-Z. Yin, W. Hu, and Y.-Q. Wei, "Compact tri-band rectangular ring patch antenna with asymmetrical strips for WLAN/WiMAX applications," *Journal of Electromagnetic Waves and Applications*, Vol. 24, No. 13, 1829-1838, 2010.
- [13]. Li, Z. Q., C. L. Ruan, L. Peng, and X. H. Wu. "Design of a simple multi-band antenna with a parasitic C-shaped strip," *Journal of Electromagnetic Waves and Applications*, Vol. 24, No. 14-15, 1921-1929, 2010.
- [14]. C. Y. Pan, T. S. Horng, W. S. Chen, and C. H. Huang, "Dual wideband printed monopole antenna for WLAN/WiMAX applications," *IEEE Antennas Wireless Propag. Lett.*, vol. 6, pp. 149-151, 2007.
- [15]. Mahatthanajatuphat, C., S. Saleekaw, P. Akkaraekthalin, and M. Krairiksh, "A rhombic patch monopole antenna with modified Minkowski fractal geometry for UMTS, WLAN, and mobile WiMAX application," *Progress In Electromagnetic Research*, Vol. 89, 57-74, 2009.
- [16]. Liu, W.-C., "Optimal design of dual band CPW-fed G-shaped monopole antenna for WLAN application," *Progress In Electromagnetic Research*, Vol. 74, 21-38, 2007.
- [17]. Song, Y., Y.-C. Jiao, G. Zhao, and F.-S. Zhang, "Multiband CPW-fed triangle-shaped monopole antenna for wireless applications," *Progress In Electromagnetic Research*, Vol. 70, 329-336, 2007.
- [18]. Yang, K., H. Wang, Z. Lei, Y. Xie, and H. Lai, "CPW-fed slot antenna with triangular SRR terminated feed line for WLAN/WiMAX applications," *Electronics Letters*, Vol. 47, No. 12, 685-686, 2011.